

3-D PRESTACK PHASE SHIFT MIGRATION OF SHOT RECORDS

MARK NG¹

SHORT NOTE

INTRODUCTION

Conventional seismic processing essentially assumes a flat layered earth. In most cases this assumption is adequate, with CDP stacking and a poststack migration giving acceptable results. However, when the geology becomes more complex, conventional CDP stacking begins to have difficulties, and prestack migration should result in a better seismic image.

In the seismic processing industry, Kirchhoff's diffraction stack migration is widely used to perform 3-D prestack migration as it is computationally efficient and versatile. The implementation of the Kirchhoff migration tries to replicate the wave equation attributes. In order to achieve that, many correction factors are required, such as de-aliasing the impulse response, amplitude compensation, as well as deviation from the high frequency and far offset assumption of the RHO filter. One may find many publications on these subjects. Since the finite-difference (F-D) and phase shift methods solve the scalar wave equation in a direct way, the outputs of these migrations carry the natural properties of the wave equation, and the amplitude and phase characteristics are better preserved.

A one-pass X-Y splitting downward continuation (F-D) shot record migration has been proposed by Froidevaux (1990) to perform 3-D prestack migration, despite the fact that it is dip limiting and dispersive. The method is based on the original 2-D version of shot record migration proposed by Reshef and Kosloff (1986). In this paper, I propose to use a phase shift operator (Gazdag, 1984) instead of an F-D operator in the diffraction term so that the migration is not dip limited and is not dispersive. This is a 3-D extension to the 2-D prestack phase shift migration of shot records described by Ng (1994). In this paper, only time migration results are presented.

METHOD

The first step in the downward continuation process is the calculation of the diffraction term which collapses the diffraction hyperboloid a little bit at every depth step. The exact full 3-D wave extrapolation for the phase shift depth migration is

$$P(k_x, k_y, z + \Delta z, \omega) = P(k_x, k_y, z, \omega) \exp \left\{ i \left[\sqrt{\left(\frac{\omega}{v}\right)^2 - k_x^2 - k_y^2} - \frac{\omega}{v} \right] \Delta z \right\} \quad (1)$$

where P is the pressure, k_x and k_y are the spatial frequencies of space x and y , ω the temporal frequency, and $v(z)$ the medium velocity, a function of depth z only. When velocities $v(x, y, z)$ vary in space, the classical one-pass splitting migration method – downward continuation of in-line and cross-line at every depth step using the local velocities at that depth of that line – is needed (Brown, 1983 and Claerbout, 1985). The split 3-D wave extrapolation for the phase shift depth migration becomes,

$$P(k_x, k_y, z + \Delta z, \omega) = P(k_x, k_y, z, \omega) \exp \left\{ i \left[\sqrt{\left(\frac{\omega}{v}\right)^2 - k_x^2} - \frac{\omega}{v} + \sqrt{\left(\frac{\omega}{v}\right)^2 - k_y^2} - \frac{\omega}{v} \right] \Delta z \right\} \quad (2)$$

For time migration applications, just substitute

$$z = v \frac{\tau}{2} \quad (3)$$

into equation (1) or (2), where τ is the 2-way output time. These equations are widely used in 3-D zero offset phase shift migration. However, in this paper, I use equations (2) and (3) as the diffraction term of the 3-D prestack phase shift time migration. Advantages of using X-Y splitting are not only the ability to adapt to lateral velocity change for the phase shift operator, but also increased programming and data management efficiency because a 2-D algorithm can be used directly in both directions. Thus, the 2-D prestack phase shift plus interpolation algorithm of Ng (1994) can be easily applied to 3-D. Since the X-Y splitting

Manuscript received by the Editor September 20, 1996; revised manuscript received October 7, 1996.

¹Geo-X Systems Ltd., 900, 425 - 1st Street S.W., Calgary, Alberta T2P 3L8 Tel: (403) 298-5600, Fax: (403) 264-1057, E-mail: markng@geo-x.com

I thank AMBER Energy for letting me show their real data example. Thanks are given to Geo-X Systems for allowing me to dedicate my time to publishing this work.

method is done only in two directions (in-line and cross-line direction), azimuthal anisotropy can be a problem for migrating steep dips, even for the 90-degree phase shift migration algorithm. That means there is a travel time error in the directions other than along the X-Y axes, and this error is at a maximum along the diagonal axes. There are two possible ways of correcting the azimuthal anisotropy: Ristow (1980) uses multidirectional splitting and Li (1991) uses a correction filter in the 3-D frequency domain to minimize the error. Either method adds some complexity to the algorithm.

The evanescent regions, where the square roots in equation (2) become negative, are handled differently than in the F-D method where they are untreated. In the phase shift method, they are zeroed, and as a result, noise reduction is provided to the section during migration. A word on the noise reduction techniques: a lot of the techniques are derived from a signal processing standpoint rather from a wave equation standpoint (Ng, 1990).

The second step in the downward continuation process after the diffraction term is applied at every depth step in the depth migration is the thin lens correction. It is essentially applying time shifts to every partially migrated trace in the data volume. It compensates for the ray bending effect as the waves travel through complicated structures:

$$P_{new}(x, y, z + \Delta z, \omega) = P(x, y, z + \Delta z, \omega) \exp \{-i\omega\delta(x, y)\} \quad (4)$$

where

$$\delta(x, y) = \left(\frac{1}{\overline{v(z)}} - \frac{1}{v(x, y, z)} \right) \frac{\Delta z}{\sqrt{2}} \quad (5)$$

and $\overline{v(z)}$ is the mean value of velocity $v(x, y)$ at depth z . The

thin lens term is very sensitive to velocity. However, in time migration, the thin lens term is ignored.

The third step involved in the downward continuation process is the imaging condition. The fully migrated output $q(x, y, z)$ or $q(x, y, \tau)$ at a particular depth or time step, depending on whether depth or time migration, is extracted from the migrated wavefield data volume $p(x, y, z, t^*)$ at the time surface t^* where the source direct wave and the reflected wave are coincident (Claerbout, 1971). The output image is

$$q(x, y, z) = p(x, y, t^*) \quad (6)$$

$$t^* = t_d + t_r \quad (7)$$

where t^* is the imaging time surface, t_d the direct arrival traveltimes from the source to the point (x, y, z) to be imaged, and t_r the traveltimes from the receiver at $(x, y, z = 0)$ to the image point (x, y, z) . Many publications exist on the subject of finding the direct arrival traveltimes t_d . It is by itself a vast subject of interest because all prestack migration algorithms need it. One may use an F-D scheme to solve for the eikonal equation (Qin et al., 1992) or detect the first arrival time from the forward modeling of the shot. Here, I just use a simple speedy approximation to obtain t_d and t_r : for depth migration,

$$t_d = \frac{\sqrt{x^2 + y^2 + z^2}}{V_{rms}(x, y, z)} \quad (8)$$

$$t_r = \frac{z}{V_{avg}(x, y, z)} \quad (9)$$

and for time migration,

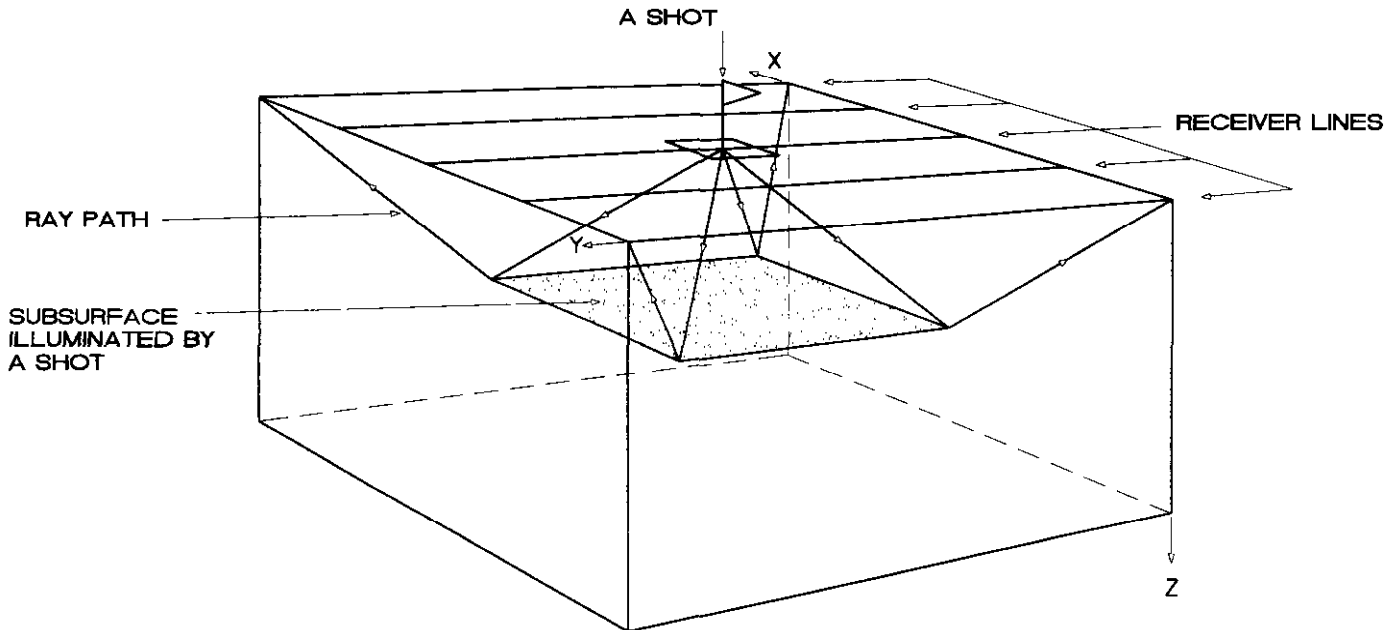


Fig. 1. Schematic of prestack shot migration. (a) A 3-D shot illuminating a subsurface.

$$t_d = \sqrt{\left(\frac{x}{V_{rms}(x,y,\tau)}\right)^2 + \left(\frac{y}{V_{rms}(x,y,\tau)}\right)^2 + \left(\frac{\tau}{2}\right)^2} \quad (10)$$

$$t_r = \frac{\tau}{2} \quad (11)$$

where V_{rms} is the root-mean-square (rms) velocity over depth and $V_{avg}(x,y,z)$ is the average velocity over depth down to the image point. Equations (8) to (11) will work satisfactorily in geology that is not too complex.

IMPLEMENTATION

Figure 1a is a schematic of a 3-D shot illuminating a subsurface flat reflector. The receivers of the 3-D shot are binned into the surface bin locations without velocity correction applied to them as shown in Figure 1b. Note that the output bin size is usually the CDP bin size but is not restricted to be so. The rest of the bins are zeroed. Data interpolation or bin sharing is not required in the prestack phase shift migration. However, in the prestack F-D migration, a mild bin sharing of one adjacent bin before migration may be required to suppress its migration noise as the F-D operators

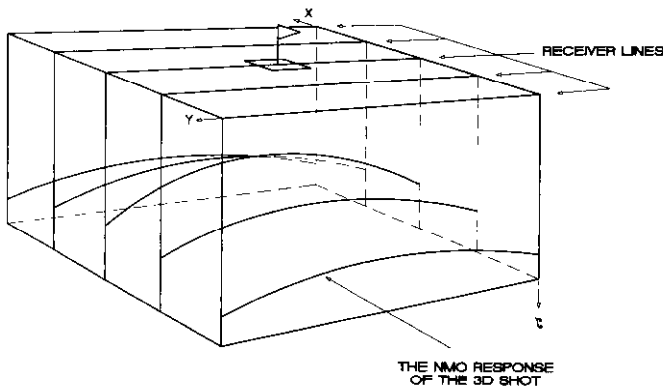


Fig. 1 (b). Binning of receivers.

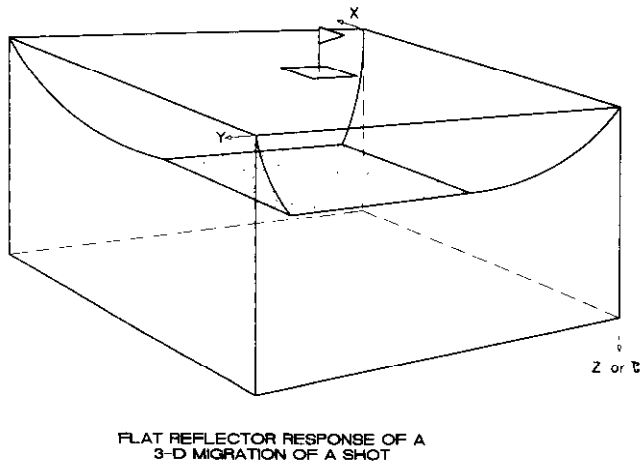


Fig. 1. (c). The subsurface flat reflector is imaged after the 3-D shot migration.

cannot handle excessively high spatial frequency data. The shot is then migrated, and the subsurface reflector will be in the illuminated position as shown in Figure 1c. Then all the migrated shots are muted and stacked to reconstruct the final output. A synthetic data example is given in Example 1.

DATA EXAMPLES

Example 1

The purpose of this example is to illustrate how a single shot of 3-D prestack F-D and prestack phase shift migration respond to a flat subsurface reflector. The synthetic shot illuminating a subsurface flat reflector at 500 ms contains 360 traces, and it is generated based on a real land data geometry with a shot patch of 9 receiver lines. The receiver line separation distance varies with an average of 250 m, with a 50 m receiver interval. The CDP bin size is 25 by 25 m. The velocity is 3000 m/s. The results of the prestack migrations with a downward continuation time step of 20 ms are shown in Figure 2. The shot S position is at in-line 45, cross-line 61. The result of the migrations is not a single clean flat surface but 9 quasi-ellipsoids which bottoms touch the flat reflector position at 500 ms. This is only one shot, one fold data. Multi shots from different locations covering a wide range of azimuths are needed to reconstruct the subsurface flat

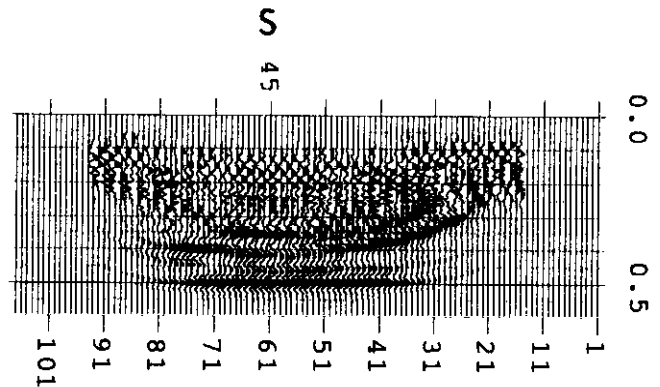


Fig. 2. 3-D prestack shot migration responses to a flat reflector. (a) Prestack F-D migration result: in-line 45.

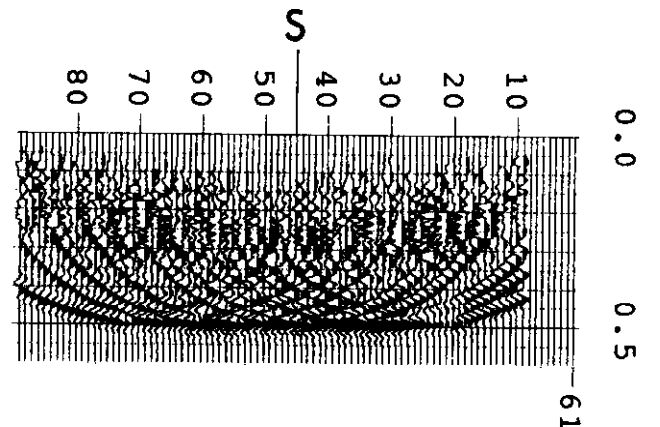


Fig. 2 (b). Prestack F-D migration result: cross-line 61.

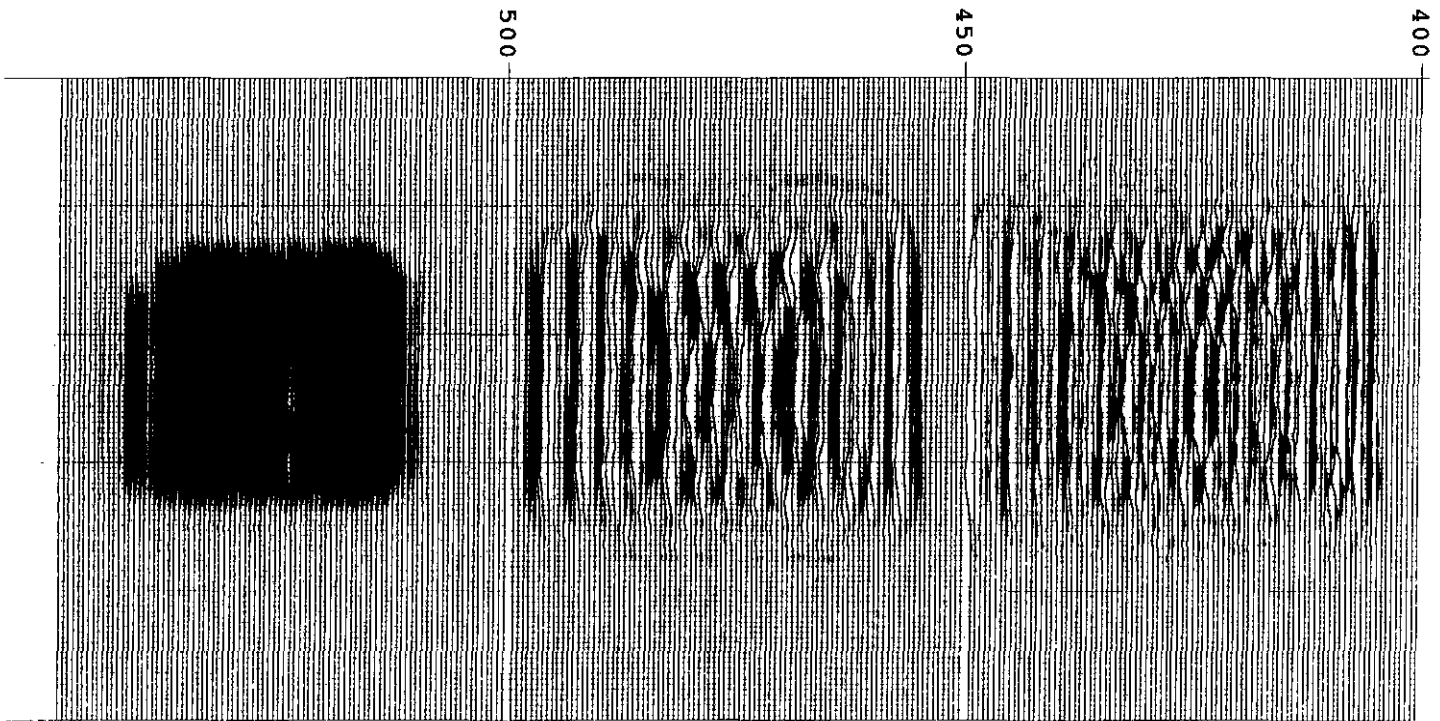


Fig. 2 (c). Prestack F-D migration result: time slices at 500, 450, 400 ms.

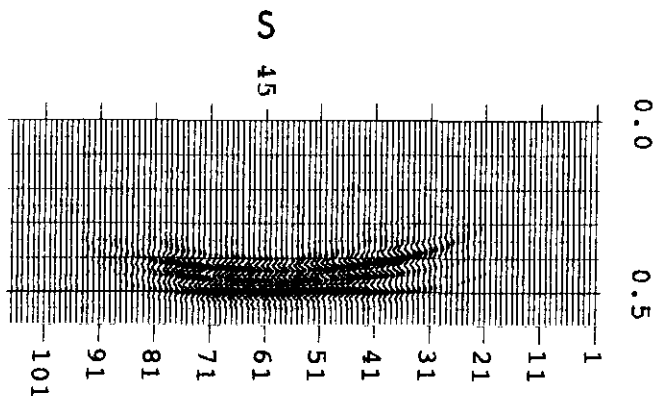


Fig. 2 (d). Prestack phase shift migration result: in-line 45.

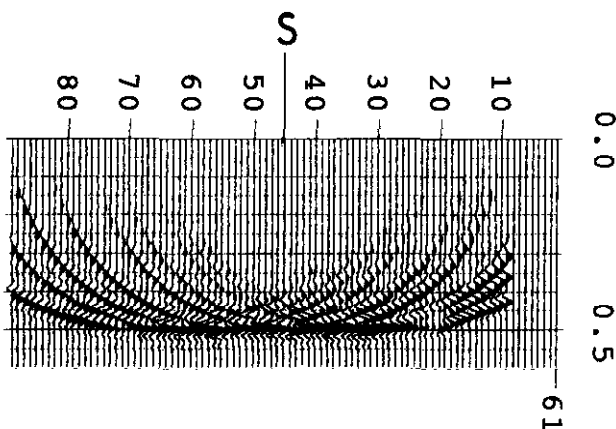


Fig. 2 (e). Prestack phase shift migration result: cross-line 61.

reflector. It is evident in the in-line, cross-line and time slice displays that the phase shift migration results (the smiles) shown in Figure 2d, 2e, 2f are cleaner and more sharply focused than those of the F-D shown in Figure 2a, 2b, 2c.

Example 2

Figure 3 shows the non-zero offset impulse response of the 65-degree 3-D prestack F-D migration and of the prestack phase shift migration. The distance between the shot S and geophone receiver G is 500 m. The impulse is at 527 ms beneath the receiver position. The CDP bin size is 25 by 25 m with a velocity of 3000 m/s. The downward continuation time step used is 20 ms. Note that in Figure 3a and 3c the bottom of the impulse response of either migration is at 500 ms in the mid-point position between the shot and receiver positions instead of at the receiver position at a deeper time, 527 ms, where the impulse was originally positioned. The prestack phase shift migration impulse response in Figure 3c and 3d have overall better amplitude behaviour than that of the F-D method in Figure 3a and 3b. This can be seen more clearly at the steep dip regions where the phase shift method gives good amplitude response up to 90 degrees dip. The time slices at 350 ms of both prestack migration methods are shown in Figure 3b and 3d, and both have an oval shape. The dip angle at the top and bottom of the oval is in the vicinity of 45 degrees dip. Note that the size of the oval of the F-D method (Figure 3b) is smaller than that of the phase shift (Figure 3d). The size of the impulse response of the F-D method (Figure 3a) becomes smaller than that of the phase shift method (Figure 3c) as dips become steeper in the

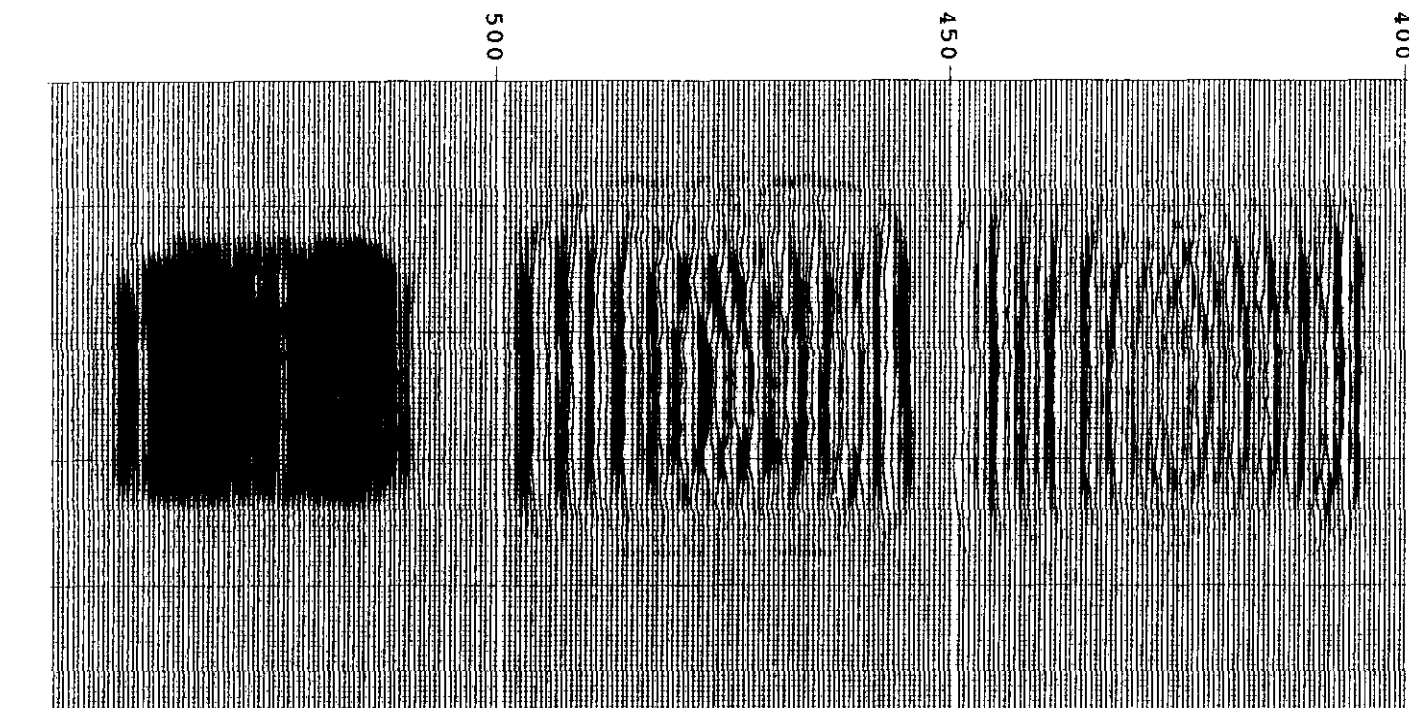


Fig. 2 (f). Prestack phase shift migration result: time slices at 500, 450, 400 ms.

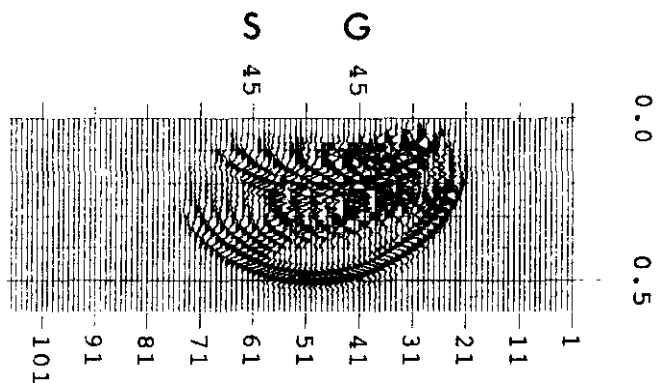


Fig. 3. Impulse response. (a) Prestack F-D migration result: in-line 45.

shallow time. This is due to the dip limitation of the 65-degree F-D algorithm. Dispersion is also apparent in the F-D method (Figure 3a). As a result, the F-D method can cause phase distortion to the output migration even for flat data. Furthermore, the F-D method in Figure 3a shows strong evanescent energy in the middle of the curve while the phase shift method in Figure 3c shows none. A good impulse response is the basis of any good migration process.

Example 3

The results of a real data set processed by 3-D poststack F-D, poststack phase shift, prestack F-D and prestack phase shift are shown in Figures 4, 5, 6 and 7 respectively in which the in-line result is in the corresponding figure a, cross-line in figure b and time slice in figure c. This land data was

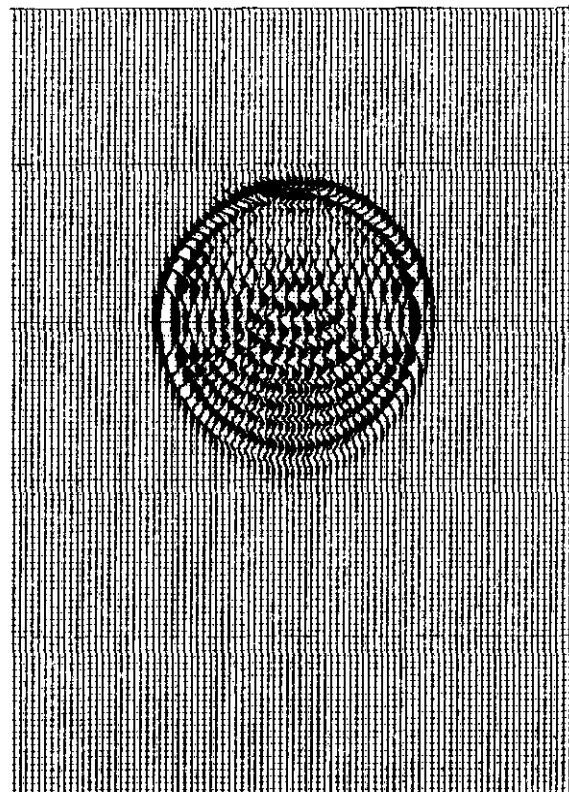


Fig. 3 (b). Prestack F-D migration result: time slice at 350 ms.

acquired with a typical 3-D geometry of 240 shots, a total of 7 shot lines with an average of 390 m line separation. Shot lines and receiver lines are perpendicular to one another. Each shot contains a 390-trace patch of 10 receiver lines with

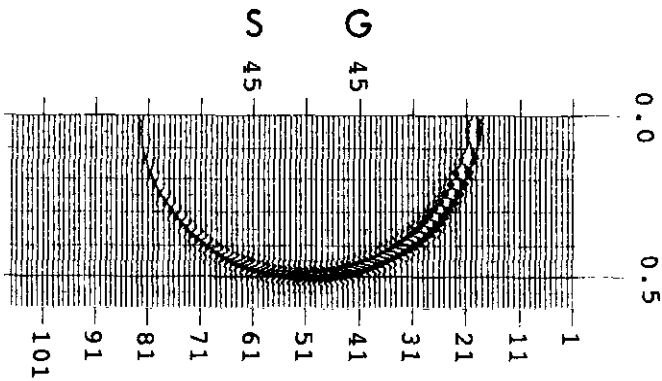


Fig. 3 (c). Prestack phase shift migration result: in-line 45.

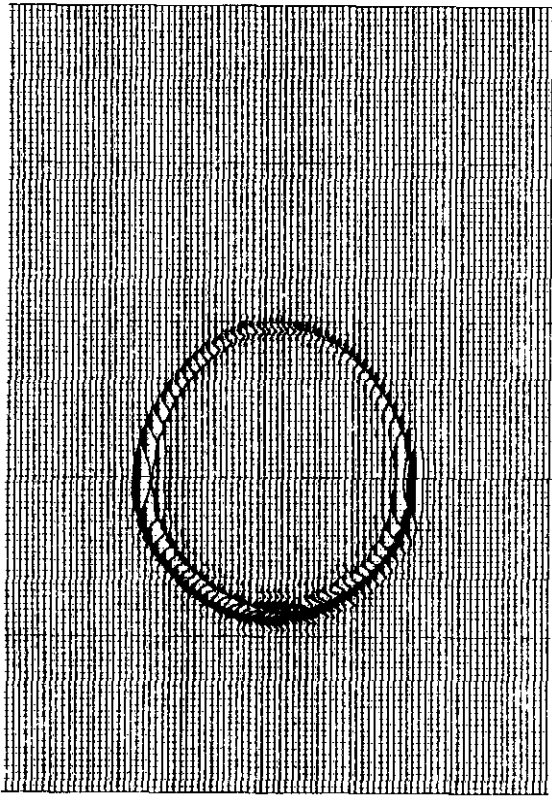


Fig. 3 (d). Prestack phase shift migration result: time slice at 350 ms.

an average of 270 m line separation. The receiver interval is 60 m, and the CDP bin size is 30 by 30 m.

A 20 ms downward continuation time step using processing velocities is used in the prestack migrations. In comparing the results between prestack and poststack migration, prestack migration methods by both F-D and phase shift in general give better results than those of the poststack counterparts in terms of signal-to-noise ratio and reflector continuities, as for example the in-line reflector at time 920 ms in Figure 4a, 5a, 6a, 7a. Other than that, the flank of the reef edge, where a successful oil well was drilled at around 1020 to 1050 ms, is clearly imaged by both prestack migration methods (Figure 6a and 7a) whereas both poststack migration counterparts (Figure 4a and 5a) just show a hint of the

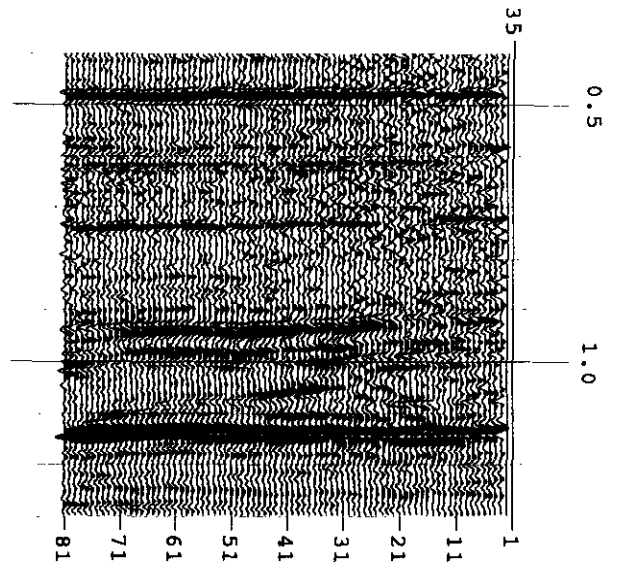


Fig. 4. Poststack F-D migration of a real 3-D data set. (a) In-line 35.

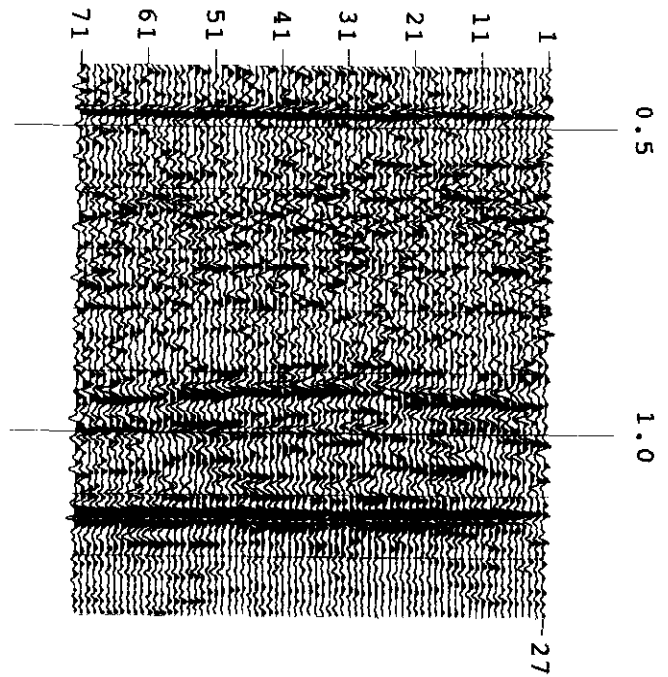


Fig. 4 (b). Cross-line 27.

reef edge. The time slices of both prestack migration methods (Figure 6c and 7c) focus the reef contour more sharply than those of the poststack migration methods (Figure 4c and 5c), and the shape is slightly different.

In comparing the results between the prestack F-D (Figure 6) and prestack phase shift (Figure 7) migration, one may notice that the phase shift migration gives a further signal-to-noise improvement. For example, reflectors at around 550 to 750 ms in the cross-line of the prestack phase shift migration (Figure 7b) are better defined than those of the prestack F-D migration (Figure 6b) and are substantially better than those of the poststack migration results (Figure 5b, 4b) which do not show much at all. A phase error can be observed in the



Fig. 4 (c). Time slice at 1064 ms.

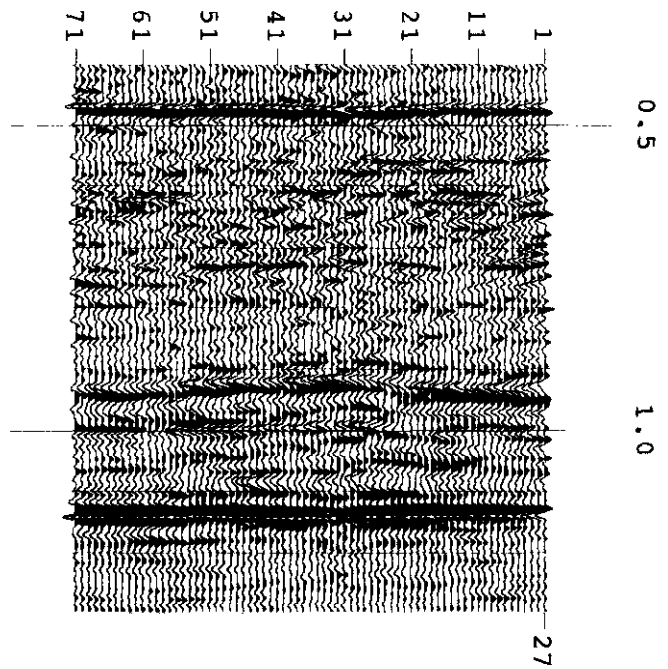


Fig. 5 (b). Cross-line 27.

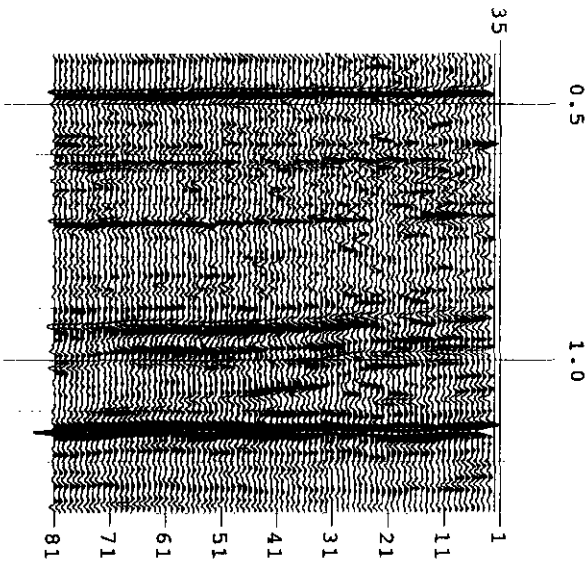


Fig. 5. Poststack phase shift migration of a real 3-D data set. (a) In-line 35.

doublers at 900 and 980 ms in the cross-line of the prestack F-D migration in Figure 6b but not in the prestack phase shift migration in Figure 7b when compared to the poststack migration results. This phase distortion is due to the dispersion and dip limitation of the 65-degree F-D algorithm as explained in Examples 1 and 2 in that even flat geologies are being migrated in prestack migration.

Although the improvements are incremental from poststack F-D migration (Figure 4) to poststack phase shift migration (Figure 5), then to prestack F-D migration (Figure 6) and then to prestack phase shift migration (Figure 7), there



Fig. 5 (c). Time slice at 1064 ms.

is a substantial improvement from poststack F-D migration (Figure 4) to prestack phase shift migration (Figure 7).

DISCUSSION AND CONCLUSIONS

Since the proposed algorithm is essentially a 3-D shot migration where each shot is migrated independently, shots can be prestack migrated in parallel by separate CPUs to increase the throughput. Like any other prestack migration

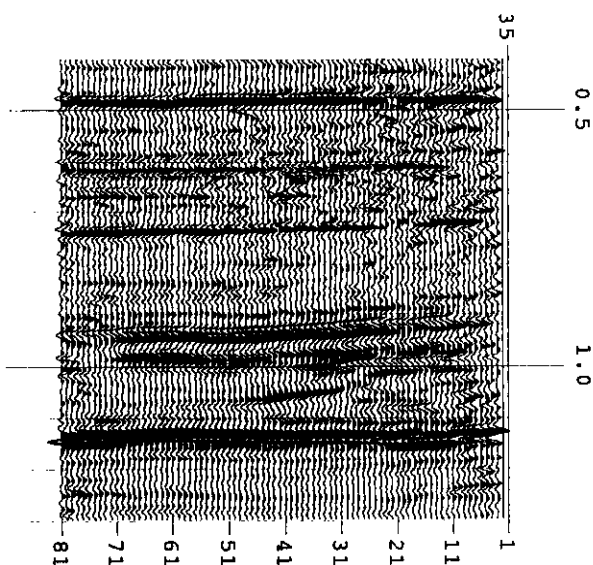


Fig. 6. Prestack F-D migration of a real 3-D data set. (a) In-line 35.

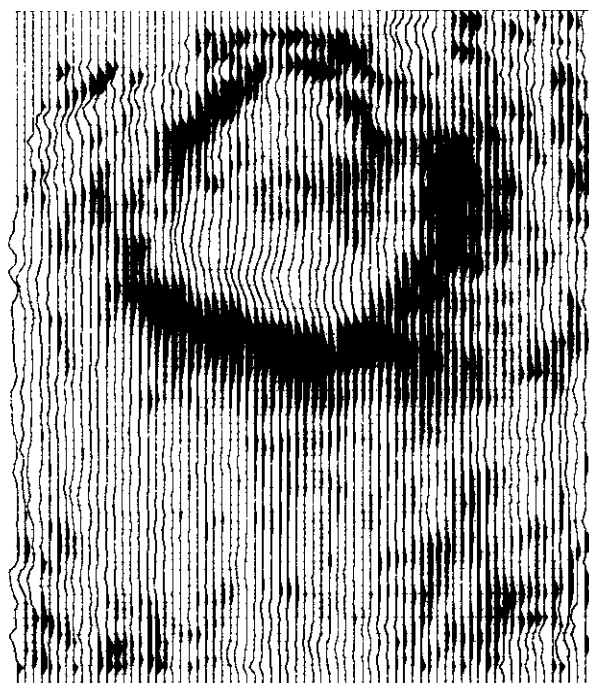


Fig. 6 (c). Time slice at 1064 ms.

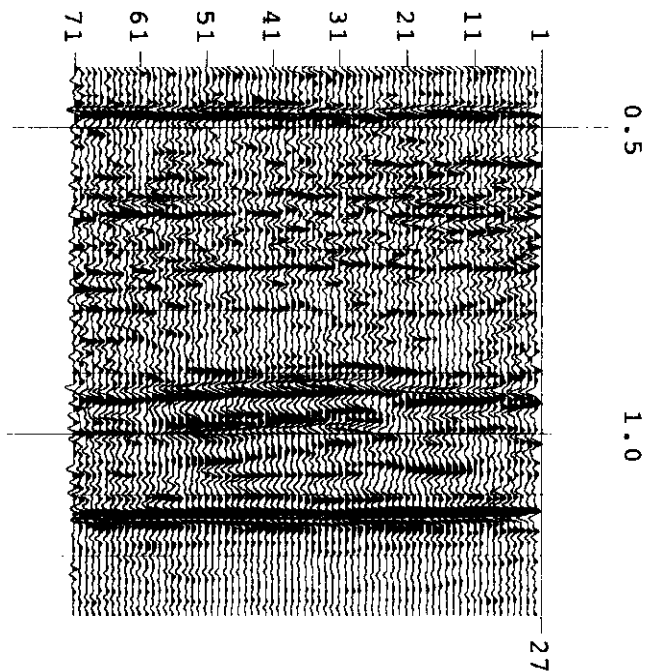


Fig. 6 (b). Cross-line 27.

methods, 3-D prestack phase shift migration needs multi shots, multi azimuths and the continuum of the wavefield to reconstruct the migrated subsurface. In conventional processing, a zero offset stack continuum is constructed before the poststack migration is applied, but in prestack migration processing it does not have that benefit. Experience shows that in regular well sampled surveys, a 3-D prestack migration gives better images than does a poststack migration, but in poorly sampled surveys, it gives worse results with more migration artifacts. By no means is a 3-D prestack migration a remedy for a poorly spatially sampled shooting. Unfortunately, I have not quantified this observation. It would be highly desirable if the acquisition requirements for

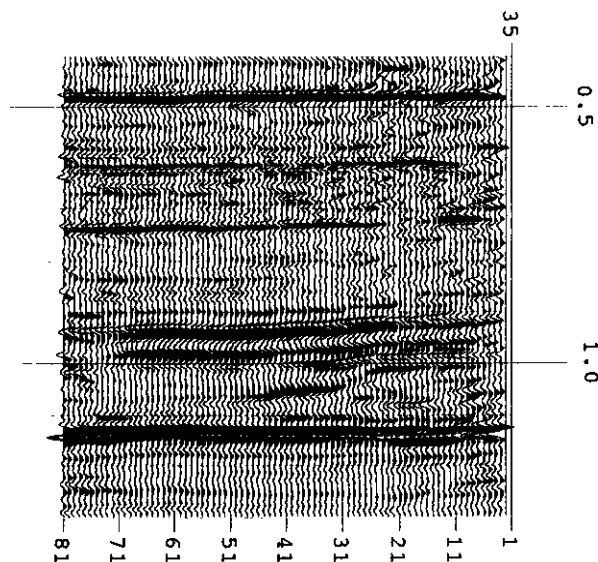


Fig. 7. Prestack phase shift migration of a real 3-D data set. (a) In-line 35.

a good 3-D prestack migration could be quantified in the future. A helpful essay addressing this problem can be found in Canning et al. (1996).

The use of a phase shift operator in the diffraction term of a 3-D prestack shot migration does improve the quality of the migration compared to the existing F-D algorithm. The method is not dip limited, nor dispersive. It gives few migration artifacts and good signal-to-noise. The one pass X-Y splitting method allows a simple direct application of the 2-D prestack phase shift migration. Since the prestack phase shift migration solves the wave equation directly, it bears all the wave equation attributes naturally.

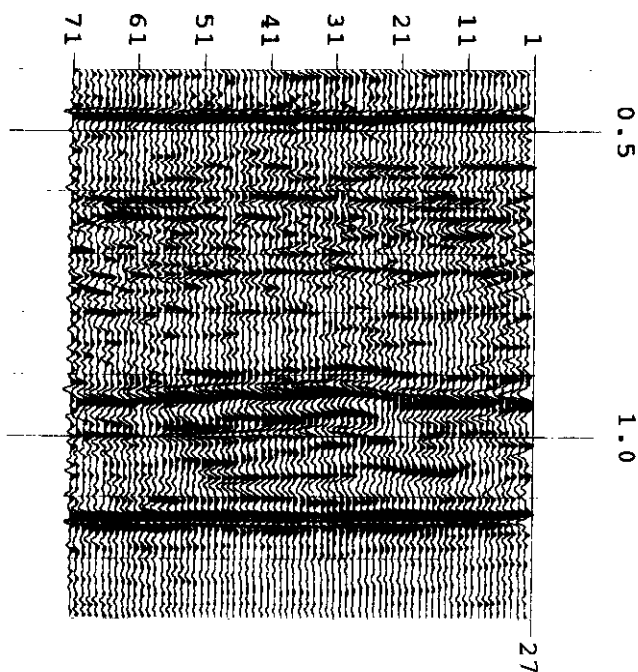


Fig. 7 (b). Cross-line 27.

REFERENCES

- Brown, D.L., 1983, Applications of operator separation in reflection seismology: *Geophysics*, **48**, 288-294.
- Canning, A. and Gardner, G.H.F., 1996, Another look at the question of azimuth: *The Leading Edge*, **15**, 821-823.
- Claerbout, J.F., 1971, Toward a unified theory of reflector mapping: *Geophysics* **36**, 467-481.
- _____, 1985, *Imaging the earth's interior*: Blackwell Scientific Publications.
- Froidevaux, P., 1990, First results of a 3-D prestack migration program: 60th Ann. Internat. Mtg., Soc. Expl. Geophys., Expanded Abstracts, 1318-1321.
- Gazdag, J. and Sguazzero, P., 1984, Migration of seismic data by phase shift plus interpolation: *Geophysics* **49**, 124-131.



Fig. 7 (c). Time slice at 1064 ms.

- Li, Z., 1991, Compensating finite-difference errors in 3-D migration and modeling: *Geophysics*, **56**, 1650-1660.
- Ng, M., 1990, Noise reduction methods – a tutorial: *Can. Soc. Expl. Geophys., The Recorder* **15**, no. 4, 8-33.
- _____, 1994, Prestack migration of shot records using phase shift plus interpolation: *Can. J. of Expl. Geophys.* **30**, 11-27.
- Qin, F., Luo, Y., Olsen, K.B., Cai, W. and Schuster, G.T., 1992, Finite-difference solution of the eikonal equation along expanding wavefronts: *Geophysics*, **57**, 478-487.
- Reshet, M and Kosloff, D., 1986, Migration of common shot gathers: *Geophysics* **51**, 324-331.
- Ristow, D., 1980, 3-D downward extrapolation of seismic data in particular by finite difference methods: Ph.D. thesis, Univ. of Utrecht, The Netherlands.